



Effect of Deflected Membrane Electrode Assembly on Species Distribution in PEMFC

A.Torkavannejad^{*a}, M.pesteei^a, M. Khalilian^a, F. Ramin^b, I.Mirzaee^a

^a Department of Mechanic, University of Urmia, Urmia, Iran

^b Department of Mechanic, University of Tabriz, Tabriz, Iran

PAPER INFO

Paper history:

Received 05 July 2013

Received in revised form 09 March 2014

Accepted 26 June 2014

Keywords:

Deflection

Fuel Cell Performance

PEM Fuel Cells

Single-Phase

ABSTRACT

This article presents the results of a numerical study, using computational fluid dynamics (CFD) analysis to investigate the species distribution of proton exchange membrane fuel cells (PEMFCs) with deflected membrane electrode assembly (MEA). These new geometry were examined while employing three-dimensional, single phase, non-isothermal and parallel flow for model of a PEM fuel cell. This numerical research has concentrated on the effect of new kind of deflected MEA while maintaining the same inlet and boundary condition. Initially, the CFD result of polarization curve has been validated with the available experimental data and shown good concord; then, studied deflected and flatted MEA at cathode and anode side. Investigation showed better results for the PEMFC with having both flatted and deflected MEA at cathode side than base model because of having more reacting area, uniform distribution of reactants, better oxygen transportation to the GDL at shoulder region and having less Cathode Overpotential (COP) which is the main causes of losses.

doi: 10.5829/idosi.ije.2015.28.03c.18

NOMENCLATURE

a	Water activity
C	Molar concentration (mol/m ³)
D	Mass diffusion coefficient (m ² /s)
F	Faraday constant (C/mol)
I	Local current density (A/m ²)
j	Exchange current density (A/m ²)
k	Permeability (m ²)
m	Molecular weight (kg/mol)
nd	Electro-osmotic drag coefficient
p	Pressure (Pa)
R	Universal gas constant (J/mol-K)
T	Temperature (K)
t	Thickness
X	Mole fraction

Greek Symbols

λ_{eff}	Effective thermal conductivity (w/m-k)
α	Effective porosity
σ_e	Membrane conductivity (1/ohm-
η	Over potential (v)
λ	Water transfer coefficient)
ρ	Density (kg/m ³)
μ	Viscosity (kg/m-s)
ζ	Stoichiometric ratio

Subscripts

MEA	Membrane electrolyte assembly
ch	Channel
a	Anode
c	Cathode
cl	Catalyst
GDI	Gas diffusion layer

*Corresponding Author's Email: ashkantorkavannejad@yahoo.com (A. Torkavannejad)

Please cite this article as: A.Torkavannejad, M.pesteei, M. Khalilian, F. Ramin, I.Mirzaee, Effect of Deflected Membrane Electrode Assembly on Species Distribution in PEMFC, International Journal of Engineering (IJE), TRANSACTIONS C: Aspects Vol. 28, No. 3, (March 2015) 467-475

1. INTRODUCTION

Fuel cells are electrochemical devices that change chemical energy of reactants, directly into electrical energy. The important features of fuel cell that sharply increased the appeal of fuel cells in generating electricity include: high performance, not being limited to Carnot cycle, silent and long term operation, and not having problems of emission control and waste disposal. These advantages make the fuel cells attractive choices for the replacement to internal combustion engines [1]. High cost of launch and economical cost is the major disadvantage of fuel cells. Different types of fuel cells have been developed, which are distinguished by the electrolyte used. Among all kinds of fuel cells, proton exchange membrane fuel cell (PEMFC) has been considered as a principle candidate for future transportation application as well as for small devices such as laptop. In these fuel cells, fuel (e.g., hydrogen gas) and an oxidant (e.g., oxygen gas from the air) are used to generate electricity, while heat and water are unavoidable products of the fuel cell operation. A fuel cell typically works on the following principle: as the hydrogen gas flows into the fuel cell on the anode side, a platinum catalyst facilitates oxidation of the hydrogen gas which produces protons (hydrogen ions) and electrons. The hydrogen ions diffuse the MEA. The electrons, which cannot pass through the membrane, flow from the external electrical circuit for energy consumption. At the cathode side, oxygen molecules combine with hydrogen ions and produce water and heat.

The anode and the cathode (the electrodes) are porous and made of an electrically conductive material, typically carbon. The faces of the electrodes in contact with the membrane contain. The PEM electrodes are kind of gas-diffusion type and generally designed for maximum surface area per unit material volume.

In recent years, researchers pay more attention to modeling and simulation of different aspects in PEMFCs with a view to enhance the cell performance and optimize the cost. In this way, a great number of researches have been conducted to improve the performance of PEMFC. Among these studies, various operating condition have been examined [2-10]. Another major issue that researchers focus more for commercialization of these cells, is the geometrical design of PEMFC. One of the geometrical parameters that affect the fuel cells is the shoulder width. It has been found that cells with smaller shoulder width are better than those with larger shoulder width due to more uniform distribution of reactants [11-15].

Other geometries have been investigated to increase permeability of reactants by using obstacle in channel area [16] and different channel geometries [17-20]. Various serpentine flow fields have been examined for

reaching higher output [21-24]. D.H. Ahmed et al. [25] performed simulations of PEMFCs with a new design for the channel shoulder geometry, in which the MEA is deflected from shoulder to shoulder. F. Arabi et al. investigated the effect of an innovative bipolar plate on PEMFC performance [26].

In the present study, three-dimensional, single phase, isothermal and parallel flow model of a PEM fuel cell with deflected membrane electrode assembly (MEA) was performed which deflected in both anode and cathode side, respectively. These geometries were used with single straight channel geometry while maintaining the same boundary conditions and inlet area and including humidification for both anode and cathode. This new geometry was designed to improve the reactant distribution and improve the cell performance. The numerical results showed that deflection toward cathode side gives higher current density at the same voltage than the contrary side.

In this work, MEA materials were examined for deflection and could be deflected up to optimum elastic limit [27].

The simulation results were validated by comparison with results in the literature and showed good concord with experimental data. Detailed analyses of the fuel cell behavior under various deflection values are discussed in the following sections.

2. MODEL DESCRIPTION

2. 1. System Description Constant mass flow rate at the channel, inlet constant pressure condition at the channel outlet, and no-flux conditions are executed for mass, momentum, species and potential conservation equations at all boundaries expect for inlets and outlets of the anode and cathode flow channels.

The side faces are symmetrical, while in the experimental sets, the fuel cell has three mono cells.

For the Layers where the electro chemical reactions occur, the meshes are finer. Also, grid independence test was implemented and finally the optimum number of meshes (164 000) was chosen. Figure 2 indicates the computational domain of base model. The cell consists of hydrogen and oxygen channels, bipolar plates on cathode and anode side of cell, which function as current collector with high electronic conductivity and the membrane electrode assembly (MEA) is located between gas channels.

2. 2. Model Assumption Non-isothermal model is assumed to perform in steady manner under constant load conditions. All gases are assumed to obey ideal gas behaviors. GDLs and catalyst layers are homogeneous and isotropic porous mediums. Flow is incompressible

and laminar due to the low pressure gradients and velocities. Volume of liquid-phase water produced in electrochemical reactions is negligible and phase change or two phase-transports are not considered, so this model is considered as a single phase. The membrane is impermeable to cross-over of reactant gases and assumed to be fully humidified. The species diffusion and electrochemical reaction conform to the dilute solution theory and Butler-Volmer kinetic equation, respectively.

3. MODEL EQUATIONS

3. 1. Gas flow Fields In the fuel cell, the gas-flow field is obtained by solving the steady-state Navier-Stokes equations, i.e. the continuity equation:

$$\nabla \cdot (\rho u) = 0 \quad (1)$$

and momentum equations;

$$\begin{aligned} \nabla \cdot (\rho u \otimes u - \mu \nabla u) = \\ - \nabla \cdot \left(P + \frac{2}{3} \mu \nabla u \right) + \nabla \cdot [\mu (\nabla u)^T] \end{aligned} \quad (2)$$

The mass balance is described by the divergence of the mass flux through diffusion and convection. The steady state mass transport equation can also be written in the following expression for species i ;

$$\nabla \cdot \left[-\rho y_i \sum_{j=1}^N D_{ij} \frac{M}{M_j} \left(\nabla y_j + y_j \frac{\nabla M}{M} \right) + \rho y_i u \right] = 0 \quad (3)$$

where, the subscript i denotes oxygen at the cathode side and hydrogen at the anode side, and j is water vapor in both cases. Nitrogen is the third species at the cathode side.

The Maxwell-Stefan diffusion coefficients of any two species are dependent on temperature and pressure. They can be calculated according to the empirical relation based on the kinetic gas theory [23];

$$D_{ij} = \frac{T^{1.75} \times 10^{-3}}{P \left[\left(\sum_k V_{ki} \right)^{1/3} + \left(\sum_k V_{kj} \right)^{1/3} \right]^2 \left[\frac{1}{M_i} + \frac{1}{M_j} \right]^{1/2}} \quad (4)$$

In this equation, pressure is in [atm], and the binary diffusion coefficient is in [cm²/s]. The values for $\sum V_{ki}$ are given by Fuller et al. [27], and the temperature field is obtained by solving the convective energy equation;

$$\nabla \cdot (\rho C_p u T - k \nabla T) = 0 \quad (5)$$

3. 2. Gas Diffusion Layers Transport in the gas diffusion layer is modeled as transport in a porous media. The continuity equation in the gas diffusion layers becomes:

$$\nabla \cdot (\rho \varepsilon u) = 0 \quad (6)$$

The momentum equation reduces to Darcy's law:

$$u = \frac{K_p}{\mu} \nabla P \quad (7)$$

The mass transport equation in porous media is:

$$\nabla \cdot \left[-\rho \varepsilon y_i \sum_{j=1}^N D_{ij} \frac{M}{M_j} \left(\nabla y_j + y_j \frac{\nabla M}{M} \right) + \rho \varepsilon y_i u \right] = 0 \quad (8)$$

In order to account for geometric constraints of the porous media, the diffusivities are corrected using the Bruggemann correction formula:

$$D_{ij}^{eff} = D_{ij} \times \varepsilon^{1.5} \quad (9)$$

The heat transfer in the gas diffusion layers is governed by:

$$\nabla \cdot (\rho \varepsilon C_p u T - k_{eff} \varepsilon \nabla T) = \varepsilon \beta (T_{solid} - T) \quad (10)$$

where, the term on the right-hand side accounts for the heat exchange to and from the solid matrix of the GDL. Here, β is a modified heat transfer coefficient that accounts for the convective heat transfer in [W/m²] and the specific surface area [m²/m³] of the porous medium [28]. Hence, the unit of β is [W/m³]. The potential distribution in the gas diffusion layers is:

$$\nabla \cdot (\lambda_e \nabla \phi) = 0 \quad (11)$$

3. 3. Catalyst Layers The catalyst layer is treated as a thin interface, where sink and source terms for the reactants are implemented. Due to the infinitesimal thickness, the source terms are actually implemented in the last grid cell of the porous medium. At the cathode side, the sink term for oxygen can be written as:

$$S_{O_2} = -\frac{M_{O_2}}{4F} i_c \quad (12)$$

whereas the sink term for hydrogen is specified as:

$$S_{H_2} = -\frac{M_{H_2}}{4F} i_a \quad (13)$$

The production of water is modeled as a source terms and hence can be given as:

$$S_{H_2O} = \frac{M_{H_2O}}{2F} i_c \quad (14)$$

The generation of heat in the cell is due to entropy changes as well as irreversibility due to the activation over potential:

$$\dot{q} = \left[\frac{T(-\Delta s)}{n_e F} + \eta_{act,c} \right] i_c \quad (15)$$

The local current density distribution in the catalyst layers can be modeled by the Butler-Volmer equation:

$$i_c = i_{o,c}^{ref} \left(\frac{C_{O_2}}{C_{O_2}^{ref}} \right) \left[\exp\left(\frac{\alpha_a F}{RT} \eta_{act,c} \right) + \exp\left(-\frac{\alpha_c F}{RT} \eta_{act,c} \right) \right] \quad (16)$$

$$i_a = i_{o,a}^{ref} \left(\frac{C_{H_2}}{C_{H_2}^{ref}} \right)^{0.5} \left[\exp\left(\frac{\alpha_a F}{RT} \eta_{act,a} \right) + \exp\left(-\frac{\alpha_c F}{RT} \eta_{act,a} \right) \right] \quad (17)$$

3. 5. Boundary Conditions For the momentum conservation equation, fuel velocity is specified at each inlet of anode and cathode flow channel. The velocity is calculated based on the concept of stoichiometry, which means “the required amount of fuel at a given condition”. Boundary conditions are set as follows: constant mass flow rate at the channel inlet and constant pressure condition at the channel outlet. The inlet mass fractions are determined by the inlet pressure and humidity according to the ideal gas law. Gradients at the channel exits are set to zero. The equations for both inlets are expressed as:

$$|\vec{u}|_{in} = \frac{\zeta}{X_{H_2,in}} \frac{I_{avg}}{2F} \frac{RT_{in}}{P_{in}} \frac{A_{MEA}}{A_{ch}} \quad (21)$$

I_{avg} is the average current density at a given cell-potential. Where, R , T_{in} , P_{in} , and ζ are the universal gas constant, temperature in the inlet, pressure in the inlet, and stoichiometric ratio, respectively. The later is defined as the ratio between the amount of supplied and the amount of required reactant on the basis of the reference current density I_{avg} , accordingly.

4. NUMERICAL IMPLEMENTATIONS

For solving the equations, the simple algorithm is applied. In addition, the main procedure for discretizing the governing equations with the appropriate boundary conditions is finite volume method and implicit solver. Figure 2 shows the algorithm for numerical simulation of model equations. Numerical test results were performed to ensure that the solutions were independent of the grid size. Moreover, the computational domain is divided into about 164000 cells.

5. RESULTS AND DISCUSSIONS

To validate the numerical simulation model used in the present study, the polarization curves were compared with the experimental data presented by Wang et al. [29]. Polarization curve of present model is shown in Figure 3. This curve signifies good concord between numerical model and experimental data. Proposed models (the models with both deflected and flat MEA)

were chosen with the same reactant flow rate (by transition MEA up and down for having the same inlet area) and constant boundary conditions. The fully humidified inlet condition for anode and cathode is used. Parametric and operating conditions can be found in Table 1.

In order to improve conventional cell performance by improving the distribution of reactants over the GDL, we simulated two kinds of deflection in which the MEA deflected at shoulder area and flatted at central region of channel for anode and cathode side for decreasing the effect of concentration losses or mass transport limitations is depicted in Figure 4. Geometry of proposed models is presented in Table 2.

As mentioned, two new cases were considered in this work. The Figure 5 revealed that case with downward deflection (case 2) produce more current density than the both, base case and upward deflection (case 3).

Figures 6 and 7 show the profile of oxygen distribution at the membrane-cathode catalyst interface. It is important to note that the distribution of oxygen mole fraction depends on deflection and for which side membrane is deflected. In case 2, at the shoulder region due to easy diffuse of reactant through GDL, Oxygen molecules distribute more uniformly due to high diffusion of reactants but at base case and case 3 oxygen scarcity in the shoulder region over the reacting area leads to higher concentration losses, which is become worse in downstream region of the channel due to depletion of reactants with moving downstream.

To make any considerable differences to find out in cell performances with these cross sections, the three main losses (AOP, COP and Ohmic loss) are going to be compared at inlet and exit region of cell. According to the below equation, the cell voltage is obtained by subtracting the losses from the open circuit voltage.

$$E = V_{oc} - \eta_{cat} - \eta_{an} - \eta_{ohm}$$

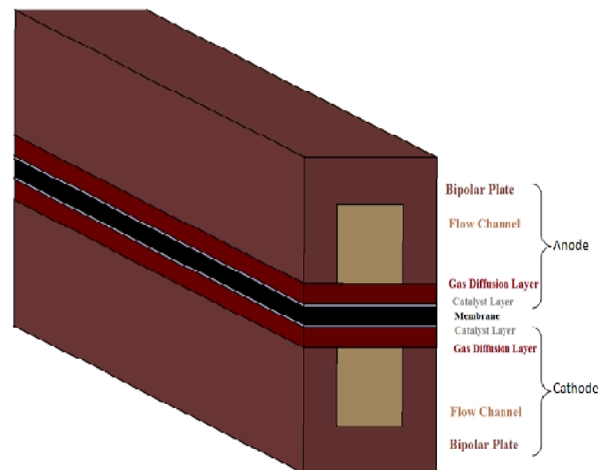


Figure 1. Computational domain of base model

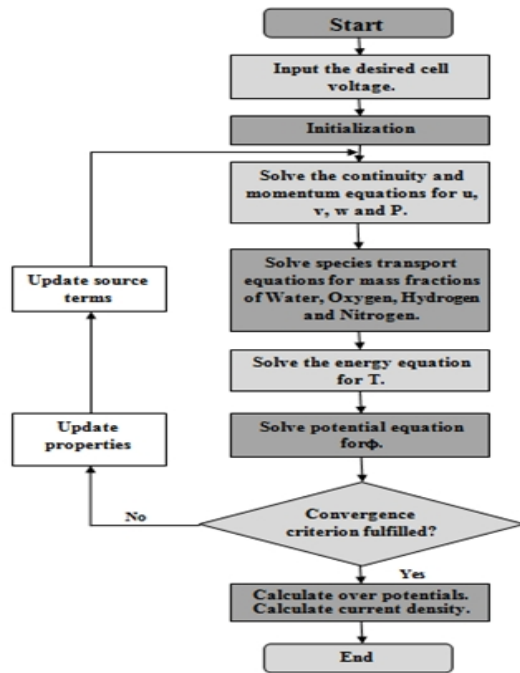


Figure 2. The algorithm for numerical simulation

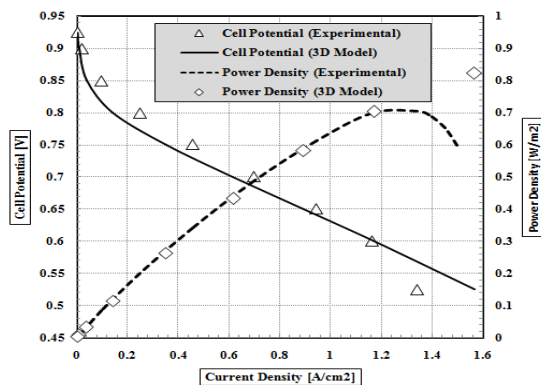


Figure 3. Comparison of polarization curve of model with experimental data

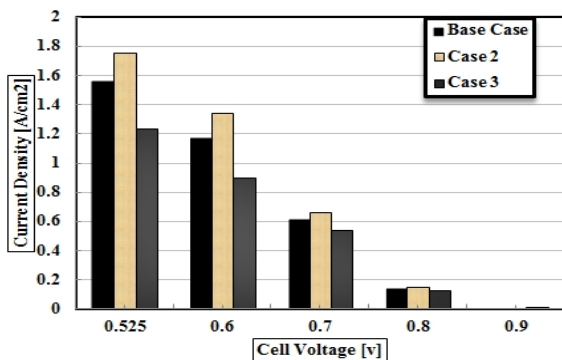


Figure 5. Comparison of performance of three numerical cases

TABLE 1. Geomeric paramets and operation condition

Parameter	Symbol	Value	Unit
Channel length	L	0.05	m
Channel width	W	1e_3	m
Channel height	H	1e_3	m
Land area width	Wland	1e_3	m
Gas diffusion layer thickness	dGDL	0.26e_3	m
Wet membrane thickness (Nafion 117)	δmem	0.23e_3	m
Catalyst layer thickness	δCL	0.0287e_3	m
Anode pressure	Pa	3	atm
Cathode pressure	Pc	3	atm
Inlet fuel and air temperature	Tcell	353.15	K
Relative humidity of inlet fuel and air (fully humidified conditions)	ψ	100	%
Refrence current density	I	10	A/cm ²
Inlet anode oxygen mass fraction	Y _{OXYGEN,A}	0	-
Inlet anode hydrogen mass fraction	Y _{HYDROGEN,A}	0.3780066	-
Inlet anode water mass fraction	Y _{WATER,A}	0.6219934	-
Inlet cathode water mass fraction	Y _{WATER,C}	0.1031307	-
Inlet cathode oxygen mass fraction	Y _{OXYGEN,C}	0.2088548	-
Inlet cathode hydrogen mass fraction	Y _{HYDROGEN,C}	0	-
Membrane equivalent weight	-	1.1	Kg/mol

TABLE 2. Geomeric paramets and operation conditions for base model

Cases	a=δ (mm)	h(membrane transition, mm)
Conventional	0	0
Downward deflection	0.25	0.1875
Upward deflection	0.25	0.1875

The COP and Ohmic loss account for the paramount reason for total losses, therefore we concentrate on analyzing them in more detail. The Ohmic loss is directly linkage to membrane thickness and local current density and inversely proportional to the membrane conductivity.

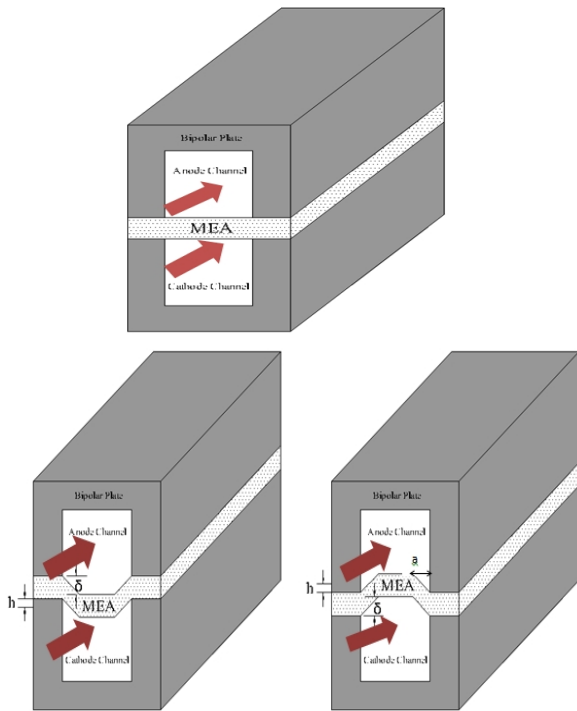


Figure 4. Conventional and new geometry with flatted and deflected MEA at cathode and anode side.

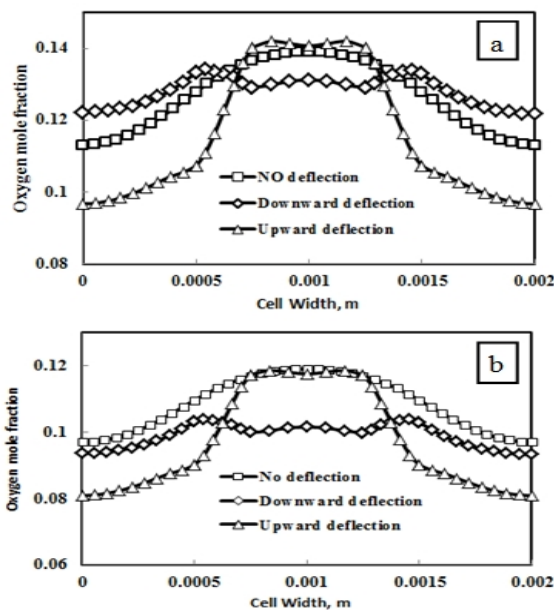


Figure 6. Comparison of oxygen mole fraction at the interface of membrane and cathode catalyst layer for three numerical models at entry (a) and exit (b) region at same voltage (0.6 volt)

The Ohmic profile is shown in Figure 8. This observation indicates that the Ohmic overpotential is higher for case 2 (downward deflection). This is because of large amount of reactants transport through

the GDL to the reacting area and led to increase the local current density, especially at shoulder region but this phenomenon is completely reverse for case 1 and case 3.

Results show that significant losses of the cell voltage occur at the cathode side. COP causes an increase in activation and concentration losses at cathode side. Inspection of the COP distribution in the fuel cell is shown in Figure 9. The cathode overpotential is mainly affected and dominated by the oxygen accessibility at the membrane–cathode GDL interface which increases significantly in the shoulder region as well as in the downstream region of the channels.

The distribution of oxygen mass fraction at the membrane–cathode catalyst interface is shown in Figures 6 and 7. In case 3, higher activation losses attribute to oxygen shortage in the shoulder region over the reacting area, which becomes worse in the downstream region of the channel due to depletion of the reactant with moving downstream. However, in case 2, this condition is completely reverse due to different oxygen distribution.

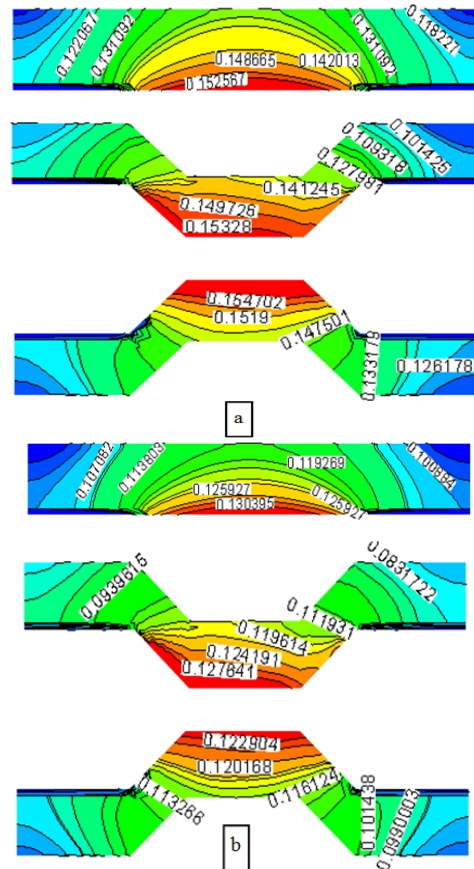


Figure 7. Countours of oxygen mole fraction at the interface of membrane and cathode catalyst layer for three numerical models at entry (a) and exit (b) region at same voltage (0.6 volt).

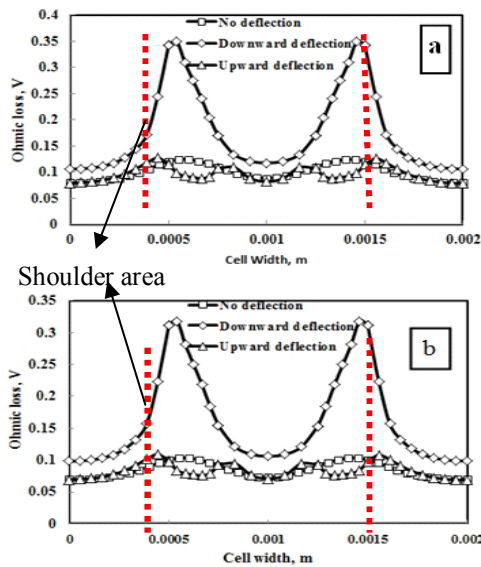


Figure 8. Comparison of Ohmic loss at the interface of membrane and cathode catalyst layer for three numerical models at entry (a) and exit (b) region at same voltage (0.6 volt).

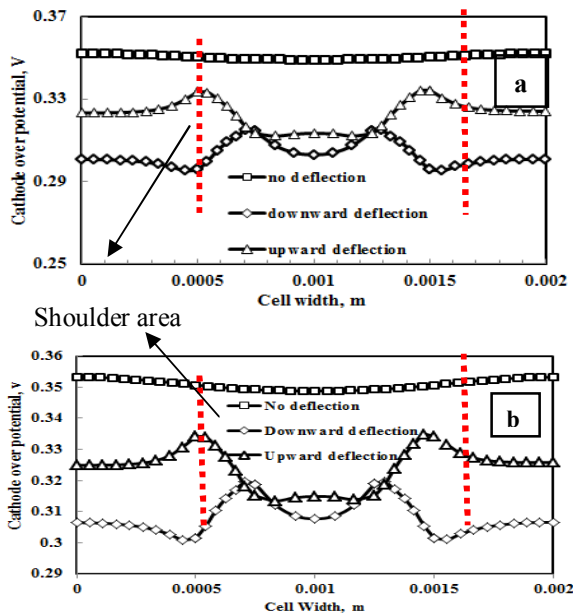


Figure 9. Comparison of cathode overpotential at the interface of membrane and cathode catalyst layer for three numerical models at entry (a) and exit (b) region at same voltage (0.6 volt).

One of the important parameters that reduce oxygen diffusivity is water. Usually, at high operating current densities, more molecules react and therefore more water is produced, which reduces the oxygen diffusivity in the cell. In general, among the three cases considered here, case 2 due to high value of oxygen and uniform

distribution led to lower cop in both channel and shoulder area.

Due to lower COP in case 2, it can be concluded that there is no critical oxygen scarcity. On the other hand, the Ohmic loss in case 2 is higher than case 3. By comparison these two losses for three cases, it is concluded that the COP had a powerful effect in reducing performance of fuel cell (in comparison with the negative effect of higher Ohmic loss).

6. CONCLUSION

In the present work, a three-dimensional computational fluid dynamics model of PEMFC with single straight flow channel has been simulated. In order to improve the cell performance, the new kind of deflection in which the MEA has been changed from conventional straight form to the waved-like form has been carried out. MEA, gives higher current density compared with two other models, due to uniformed distribution of reactants and lower value of COP.

Additionally, different types of losses were calculated for three cases. Taken altogether, comparing these losses for the three cases, this result imply that the cop and species distribution had powerful effect in reducing the fuel cell performance. Implementation of these new geometries yields more homogenous and reduced mass transport loss, as well as favoring a uniform distribution over active area and homogenous current production and high cell performance.

8. ACKNOWLEDGMENT

The financial support of the Renewable Energy Organization of Iran is gratefully acknowledged (SUNA).

9. REFERENCES

1. M. Mardi Kolor, S. Khalil Arya, Jafarmadar, S. and A. Nemati, "Hydrgen and ethanol as potential alterbative fuel compared to gasoline under improved exhaust gas recirculation.", *International Journal of Engineering*, Vol. 27, No. 3, (2014), 449-456.
2. Xing, X.Q., Lum, K.W., Poh, H.J. and Wu, Y.L., "Optimization of assembly clamping pressure on performance of proton-exchange membrane fuel cells", *Journal of Power Sources*, Vol. 195, No. 1, (2010), 62-68.
3. Chang, W., Hwang, J., Weng, F. and Chan, S., "Effect of clamping pressure on the performance of a pem fuel cell", *Journal of Power Sources*, Vol. 166, No. 1, (2007), 149-154.
4. Rho, Y.W., Srinivasan, S. and Kho, Y.T., "Mass transport phenomena in proton exchange membrane fuel cells using o 2/he, o 2/ar, and o 2/n 2 mixtures ii. Theoretical analysis", *Journal of the Electrochemical Society*, Vol. 141, No. 8, (1994), 2089-2096.

5. Amphlett, J.C., Baumert, R., Mann, R.F., Peppley, B.A., Roberge, P.R. and Harris, T.J., "Performance modeling of the ballard mark iv solid polymer electrolyte fuel cell i. Mechanistic model development", *Journal of the Electrochemical Society*, Vol. 142, No. 1, (1995), 1-8.
6. Mosdale, R. and Srinivasan, S., "Analysis of performance and of water and thermal management in proton exchange membrane fuel cells", *Electrochimica Acta*, Vol. 40, No. 4, (1995), 413-421.
7. Oetjen, H.F., Schmidt, V., Stimming, U. and Trila, F., "Performance data of a proton exchange membrane fuel cell using h₂/co as fuel gas", *Journal of the Electrochemical Society*, Vol. 143, No. 12, (1996), 3838-3842.
8. Buchi, F.N. and Srinivasan, S., "Operating proton exchange membrane fuel cells without external humidification of the reactant gases fundamental aspects", *Journal of the Electrochemical Society*, Vol. 144, No. 8, (1997), 2767-2772.
9. Uribe, F.A., Gottesfeld, S. and Zawodzinski, T.A., "Effect of ammonia as potential fuel impurity on proton exchange membrane fuel cell performance", *Journal of the Electrochemical Society*, Vol. 149, No. 3, (2002), 293-296.
10. Ticianelli, E.A., Derouin, C.R. and Srinivasan, S., "Localization of platinum in low catalyst loading electrodes to attain high power densities in spe fuel cells", *Journal of Electroanalytical Chemistry and Interfacial Electrochemistry*, Vol. 251, No. 2, (1988), 275-295.
11. Natarajan, D. and Van Nguyen, T., "A two-dimensional, two-phase, multicomponent, transient model for the cathode of a proton exchange membrane fuel cell using conventional gas distributors", *Journal of the Electrochemical Society*, Vol. 148, No. 12, (2001), A1324-A1335.
12. Lin, G. and Van Nguyen, T., "A two-dimensional two-phase model of a pem fuel cell", *Journal of the Electrochemical Society*, Vol. 153, No. 2, (2006), 372-382.
13. Lum, K.W. and McGuirk, J.J., "Three-dimensional model of a complete polymer electrolyte membrane fuel cell—model formulation, validation and parametric studies", *Journal of Power Sources*, Vol. 143, No. 1, (2005), 103-124.
14. Ahmed, D.H. and Sung, H.J., "Effects of channel geometrical configuration and shoulder width on pemfc performance at high current density", *Journal of Power Sources*, Vol. 162, No. 1, (2006), 327-339.
15. Torkavannejad, A., pesteei, m., Mirzaeei, I. and Ramin, I., "Effect of innovative channel geometry and its effect o species distribution in pemfc", *Journal of Renewable Energy and Environment*, Vol. 1, No., (2014), 20-31.
16. Ahmadi, N., Rezazadeh, S., Mirzaee, I. and Pourmahmoud, N., "Three-dimensional computational fluid dynamic analysis of the conventional pem fuel cell and investigation of prominent gas diffusion layers effect", *Journal of Mechanical Science and Technology*, Vol. 26, No. 8, (2012), 2247-2257.
17. Ge, S.-H. and Yi, B.-L., "A mathematical model for pemfc in different flow modes", *Journal of Power Sources*, Vol. 124, No. 1, (2003), 1-11.
18. Sun, L., Oosthuizen, P.H. and McAuley, K.B., "A numerical study of channel-to-channel flow cross-over through the gas diffusion layer in a pem-fuel-cell flow system using a serpentine channel with a trapezoidal cross-sectional shape", *International Journal of Thermal Sciences*, Vol. 45, No. 10, (2006), 1021-1026.
19. Guvelioglu, G.H. and Stenger, H.G., "Computational fluid dynamics modeling of polymer electrolyte membrane fuel cells", *Journal of Power Sources*, Vol. 147, No. 1, (2005), 95-106.
20. Chiang, M.-S. and Chu, H.-S., "Numerical investigation of transport component design effect on a proton exchange membrane fuel cell", *Journal of Power Sources*, Vol. 160, No. 1, (2006), 340-352.
21. Jung, H.-M., Lee, W.-Y., Park, J.-S. and Kim, C.-S., "Numerical analysis of a polymer electrolyte fuel cell", *International Journal of Hydrogen Energy*, Vol. 29, No. 9, (2004), 945-954.
22. Shimpalee, S., Lee, W.-K., Van Zee, J. and Naseri-Neshat, H., "Predicting the transient response of a serpentine flow-field pemfc: I. Excess to normal fuel and air", *Journal of Power Sources*, Vol. 156, No. 2, (2006), 355-368.
23. Weng, F.-B., Su, A., Jung, G.-B., Chiu, Y.-C. and Chan, S.-H., "Numerical prediction of concentration and current distributions in pemfc", *Journal of Power Sources*, Vol. 145, No. 2, (2005), 546-554.
24. Su, A., Chiu, Y. and Weng, F., "The impact of flow field pattern on concentration and performance in pemfc", *International Journal of Energy Research*, Vol. 29, No. 5, (2005), 409-425.
25. Ahmed, D.H. and Sung, H.J., "Design of a deflected membrane electrode assembly for pemfcs", *International Journal of Heat and Mass Transfer*, Vol. 51, No. 21, (2008), 5443-5453.
26. Arbabi, F., Roshandel, R. and Moghaddam, G.K., "Numerical modeling of an innovative bipolar plate design based on the leaf venation patterns for pem fuel cells", *International Journal of Engineering*, Vol. 25, No. 3, (2012), 177-186.
27. Fuller, E.N., Schettler, P.D. and Giddings, J.C., "New method for prediction of binary gas-phase diffusion coefficients", *Industrial & Engineering Chemistry*, Vol. 58, No. 5, (1966), 18-27.
28. Berning, T., Lu, D.M. and Djilali, N., "Three-dimensional computational analysis of transport phenomena in a pem fuel cell", *Journal of Power Sources*, Vol. 106, No. 1, (2002), 284-294.
29. Wang, L., Husar, A., Zhou, T. and Liu, H., "A parametric study of pem fuel cell performances", *International Journal of Hydrogen Energy*, Vol. 28, No. 11, (2003), 1263-1272.

Effect of Deflected Membrane Electrode Assembly on Species Distribution in PEMFC

A.Torkavannejad^a, M.pesteei^a, M. Khalilian^a, F. Ramin^b, I.Mirzaee^a

^a Department of mechanic, University of Urmia, Urmia, Iran

^b Department of mechanic, University of Tabriz, Tabriz, Iran

PAPER INFO

چکیده

Paper history:

Received 05 July 2013

Received in revised form 09 March 2014

Accepted 26 June 2014

Keywords:

Deflection

Fuel Cell Performance

PEM Fuel Cells

Single-Phase

این مقاله نتایج حاصل از یک مطالعه عددی را با استفاده از آنالیز دینامیک سیالات محاسباتی برای بدست آوردن توزیع گونه ها و افت های پیل سوختی غشا پروتونی با مجموعه غشا مورب شده را مورد مطالعه قرار دهد. این هندسه های جدید در حالی بررسی شده اند که برای مدل پیل سوختی غشا پروتونی حالت سه بعدی، تک فاز، غیر هم دما و جریان موازی به کار گرفته شده است. این پژوهش عددی روی تاثیر حالت های جدیدی از مجموعه غشا مورب شده با حفظ مساحت ورودی و شرایط مرزی متمرکز شده است. در ابتدا نتیجه CFD منحنی قطبش با داده های آزمایشی موجود که توافق خوبی نشان داده است اعتبار دهی شده و سپس مجموعه غشا دارای سطح مورب شده در هر دو طرف کاتد و آند مورد مطالعه قرار گرفته شده است. بررسی، نتایج بهتری را برای حالتی که مجموعه غشا به سمت کاتد مورب شده به دلیل داشتن منطقه واکنش بیشتر، توزیع یکنواخت تر واکنش دهنده ها، حمل اکسیژن بهتر به لایه پنخش گاز در منطقه شانه و داشتن پتانسیل اضافی کمتر در سمت کاتد که اصلی ترین تلفات متوجه آن می باشد نشان می دهد.

.doi: 10.5829/idosi.ije.2015.28.03c.18
